Spectral properties of a high quantum yield, novel aminocoumarin with a vicinal hydroxyl group

Leah H. Knoor
Calvin University
Liam P. Hoogewerf
Calvin University
Isaac B. Jonker
Calvin University
Elizabeth A. Doty
Calvin University
George R. Du Laney
Calvin University
Ronald L. Blankespoor
Calvin University
Mark A. Muyskens (mark.muyskens@calvin.edu)
Calvin University

Research Article

Keywords: Substituted coumarin, quantum yield, Stokes shift, fluorescence lifetime

Posted Date: May 11th, 2022

DOI: https://doi.org/10.21203/rs.3.rs-1608217/v1

Abstract

Knightletin is a novel, high quantum-yield, substituted coumarin in the group of fluorescent aminocoumarins. The molecule reveals the influence of a hydroxyl group on the aminocoumarin structure through its absorbance-fluorescence properties and interaction with several solvents. The substitution on the benzene ring of the coumarin affects electronic states, the molecular dipole moment and hydrogen bonding between vicinal groups as well as hydrogen bonding with solvents. This report describes the synthesis of knightletin, its absorbance-fluorescence characteristics in three solvents of varying polarity, and insights on its conformation from density functional theory modeling. The quantum yield of 0.81 in methanol is remarkable. The modeling indicates a ground state geometry with a pyramidal NH_2 group interacting with the OH in an NH-donor hydrogen bond and predicts spectroscopic characteristics consistent with the experimental observations.

Introduction

Aminocoumarins are well known to have high fluorescence quantum yields and perform well in a variety of substituted forms as commercial laser dyes [1]. This class of dyes has in common the amino group in position 7 according to the conventional coumarin numbering scheme (Scheme 1). This substituent can be unsubstituted or substituted, including cyclic structures that prevent the amine moiety from rotating. We describe for the first time a 7-aminocoumarin with a vicinal hydroxyl group: 6-hydroxy-7-amino-4-methylcoumarin, which we have given the name knightletin. This novel compound is like aesculetin, 6,7-dihydroxycoumarin, having vicinal hydrogen bonding groups on the benzene ring. However, the novel compound has a much higher quantum yield than aesculetin. Aesculetin is notable for its bioactivity and has been the subject of a recent study from our lab characterizing it as an extraordinarily strong photoacid capable of forming a complex with borate ion [2]. Besides its similarities to aesculetin, knightletin can be compared to well-studied 7-aminocoumarins that lack the hydroxyl group, such as Coumarin 120 (7-amino-4-methylcoumarin, C120) [3–5]. Interestingly, aminocoumarins are also an established class of antibiotics; in these cases, the substituted amino group is placed at position 3, with novobiocin as an example [6]. This study focuses on the photophysical properties rather than any potential bioactivity of knightletin.

The synthesis is serendipitous because the original goal of this synthetic work was to place hydroxyl groups on the coumarin structure in positions 5 and 6 so that we could study the photoacid and complex-forming behavior of vicinal dihydroxycoumarins. The target compound offers an intriguing comparison with aesculetin and with daphnetin (7,8-dihydroxycoumarin), both of which are commercially available. Knightletin––named after the mascot of Calvin University, where it was synthesized––also possesses vicinal groups that can form an intramolecular hydrogen bond, which makes it an interesting comparison to aesculetin and C120. Here we describe the synthesis of the novel aminocoumarin and characterization of its absorbance-fluorescence properties in three solvents. Future studies will examine its potential photoacid behavior and whether any species complexation occurs, such as is the case for aesculetin with borate.

Materials And Methods

The starting material for the synthesis, 4-methylgrevillone (4-methyl-6-hydroxycoumarin, compound 1a in the synthesis section), is from TCI America (Portland, OR, USA). Steady-state absorption and emission spectra were collected on a UV-Vis spectrophotometer (Hitachi U3900H) and spectrofluorometer (Horiba FluoroMax-4).

Quantum Yield Determination

A quantitative determination of the quantum yield was carried out relative to the fluorescence standard quinine sulfate (QS, 0.1 N H_2SO_4, 22°C) using 350-nm excitation for all solutions. The absolute fluorescence quantum yield of knightletin in MeCN (acetonitrile) is $\Phi_A = \Phi_Q(I_A/I_Q)(A_Q/A_A)\left(n_S/n_W\right)^2$, where Φ_Q is 0.577 for QS [7], I_A/I_Q is the ratio of the wavelength-integrated fluorescence intensity of knightletin to quinine sulfate, A_Q/A_A is the ratio of the absorbance of QS to knightletin at 350 nm, and n_S/n_W is the ratio of refractive indices of the knightletin solution solvent, in this case MeCN, and water. This analysis is performed with five absorbances over a range from 0.01 to 0.11 and yields the expected linear increase in the integrated intensity with increasing absorbance. We estimate uncertainty to be about 5% using this approach. In addition, the relative quantum yield for knightletin solutions in EtOAc (ethyl acetate) and MeOH (methanol) were compared to MeCN by determining the integrated emission intensity normalized by absorbance at the excitation wavelength. Emission spectra were recorded at the same solution concentration, excitation wavelength, excitation intensity, and emission sensitivity.

Time-resolved Fluorescence

The equipment used for time-resolved fluorescence spectroscopy has recently been described in a paper from our lab [8]. This system, used in partnership with the Blanchard group in the Department of Chemistry at Michigan State University, utilizes a picosecond laser light source. For our experiment, we used 5-ps pulses of 350-nm light and time-correlated single photon counting (TCSPC) detection. Time resolved fluorescence decays were collected for unpurged ~ 100 μM solutions of knightletin in EtOAc, MeCN, and MeOH. The effect of purging with $N_2(g)$ was tested for the knightletin/MeCN solution, purging for 10 minutes, and collecting the decay for 1.5 minutes immediately after purging; the purged decay yielded a lifetime that was about 9% longer. A study on oxygen solubility in organic solvents indicates MeCN has the highest O_2 solubility of the three selected solvents with MeOH and EtOAc being 10 and 20% lower solubility, respectively [9]. For reference, a fluorescence decay for a 100 μM solution of coumarin 1 (7-diethylamino-4-methylcoumarin) in EtOH (ethanol) collected on the same day yielded a lifetime of 3.07 ± 0.01 ns (unpurged), which agrees well with the literature report of 3.1 ns (purged) [10]. Unpurged lifetimes are reported below since purging does not appear to significantly impact the lifetime for these coumarins.

Computational Methods

All quantum chemistry modeling using density functional theory (DFT) was performed with the Gaussian 16 program package [11] and the WebMO Pro interface [12]. Full geometry optimizations of knightletin (neutral and anion) in the gas phase were performed for the ground state using the B3LYP functional and cc-pVTZ basis set. For modeling in the three solvents of this study, the SMD solvation model [13] was used as implemented in Gaussian 16 to represent a diffuse dielectric medium of the solvent. Care was taken to ensure each ground state structure was at a global minimum energy, which for the neutral structure involves comparing the intramolecular hydrogen bond with either OH or NH acting as donor. To model the excited state, the time-dependent DFT/B3LYP/cc-pVTZ method was used including the SMD solvent approach where appropriate; the predicted absorbance wavelength comes from the un-optimized and optimized excited state TD-DFT computation to model the vertical excitation and the fluorescent emission, respectively.

Synthesis Of Substituted Coumarins

The original goal of this work was the preparation of 5,6-dihydroxy-4-methylcoumarin (**1b**, see Scheme 2) for fluorescence studies on substituted coumarins with vicinal hydroxyl groups on the benzene ring akin to the more thoroughly studied 6,7-dihydroxycoumarin (aesculetin). The synthesis was accomplished using the sequence of reactions, **1a** → **1c** → **1d** → **1b**, as described in the literature by Kaufman et al. [14] Although there are reports in the literature describing the synthesis of **1c** from **1a** using HNO_3/H_2SO_4, [14, 15] no mention is made regarding its isomer **1e**, which is obtained in low yield in the nitration. Reduction of the nitro group in **1c** leads to **1d** in very good yield using dithionite, $S_2O_4^{-2}$. The last step in the sequence leading to **1b** was accomplished by treating **1d** with Fe^{+3} in aq. HCl, which results in a very low yield. Although NMR data are available in the literature for **1c** and **1e**, [16] **1f** was an unknown compound at the outset of this work.

5,6-Dihydroxy-4-methylcoumarin (1b). To a stirred solution of 0.634 g (3.28 mmol) of **1a** in 7.5 mL of 10% HCl was added 9.40 mL of 10% aq. $FeCl_3$ (3.48 mmol) over 5 min which produced a black paste. This paste was combined with 50 mL of 3:1 CH_2Cl_2 /EtOAc and the mixture was stirred with heating to dissolve **1b.** The CH_2Cl_2 /EtOAc filtrate was chromatographed on a silica gel column and eluted with the same solvent. Removal of the solvent in the eluent gave 71 mg (11%) of **1b**: mp 244–245°C (dec) (lit. mp 247–249°C) [14]; ^{1}H NMR (500 MHz, d_6-acetone) δ 8.86 (br s, 1H), 8.20 (br s, 1H), 7.10 (d, J = 8.75 Hz, 1H), 6.66 (d, J = 8.75 Hz, 1H), 6.06 (s, 1H), 2.65 (s, 3H); ^{13}C NMR (500 MHz, d_6-acetone) δ 159.9, 153.7, 148.2, 144.0, 140.3, 117.7, 113.7, 109.1, 106.4, 22.9; IR (ATR) 3131, 1644, 1609, 1596, 1564, 1473, 1364, 1307, 1269, 1197, 1060, 1036, 995, 933, 799, 637, 599, 542 cm^{-1}; HRMS (ESI) m/z $[M + H]^+$ calculated for $C_{10}H_9O_4$: 193.0501 amu; found 193.0489 amu.

6-Hydroxy-5-nitro-4-methylcoumarin (1c) and 6-hydroxy-7-nitro-4-methylcoumarin (1e). A solution of 2.92 g of 70% HNO_3 (0.0328 mmol) was added over 40 min to a solution of 5.00 g (0.0285 mmol) of **1a** in 48 mL of conc. H_2SO_4 cooled in an ice bath. The temperature was kept below 5°C during the addition. After standing in an ice-bath for 2 h, the reaction mixture was poured over 0.5 kg of ice. The yellow solid was collected by vacuum filtration and dried giving 6.28 of crude product, which produced an NMR spectrum that showed a mixture of **1c** and **1e** and a small amount of an unidentified product. The reaction mixture was introduced onto a silica gel column and eluted with 8:1 CH_2Cl_2-EtOAc to give 0.560 g (9%) of **1e** as a yellow solid: mp 191°C (dec) (lit mp 185°C)[16]; ^{1}H NMR (500 MHz, d_6-DMSO) δ 11.1 (s, 1H), 7.92 (s, 1H), 7.34 (s, 1H), 6.55 (s, 1H), 2.38 (s, 3H); ^{13}C NMR (500 MHz, d_6-DMSO) δ 159.6, 151.8, 147.8, 145.0, 139.0, 125.0, 118.0, 114.4, 113.0, 18.4; IR (ATR) cm^{-1} 3278, 1710, 1572, 1483, 1445, 1221, 1173, 930, 883, 827, 618, 582 cm^{-1}.

Elution with 4:1 CH_2Cl_2-EtOAc gave 4.62 g (74%) of **1c** as yellow crystals: mp 240–245°C (dec), (lit. mp 220–222°C)[REF RB1]; ^{13}C NMR (500 MHz, d_6-acetone) δ 11.2 (s, 1H), 7.46 (d, J = 9.15 Hz, 1H), 7.31 (d, J = 9.15 Hz, 1H), 6.52 (s, 1H), 2.22 (s, 3H); ^{13}C NMR (500 MHz, d_6-acetone) δ 158.8, 148.4, 146.2, 146.1, 135.4, 121.2, 120.3, 119.1, 112.1, 17.89; IR (ATR) 3295, 1685, 1577, 1437, 1266, 1228, 1208, 1172, 936, 857, 822, 637, 622, 574 cm^{-1}; HRMS (ESI) m/z $[M + H]^+$ calculated for $C_{10}H_8NO_5$: 222.0403 amu; found 222.0402 amu.

6-Hydroxy-5-amino-4-methylcoumarin (1d). To an ice-cold solution of 2.50 g (11.3 mmol) of **1c** in 31 mL of conc. NH_3 was added with stirring an ice-cold solution of 38.5 g (0.225 mmol) of 82% $Na_2S_2O_4$ in 150 mL of water. The reaction mixture rapidly changed color from red to yellow and, after stirring at 25°C for 3 h, a yellow solid was collected by vac. filt. and dried to give 1.62 g (75%) of **1d**: mp 257–259°C (dec) (lit. mp 253–256°C)[14]; ^{1}H NMR (500 MHz, d_6-DMSO) δ 9.56 (br s, 1H), 6.90 (d, J = 9.57 Hz, 1H), 6.46 (d, J = 9.57 Hz, 1H), 5.99 (s, 1H), 5.02 (br s, 2H), 2.62 (s, 3H); ^{13}C NMR (500 MHz, d_6-DMSO) δ 165.2, 159.8, 152.9, 146.0, 140.3, 121.7, 117.3, 112.9,108.8, 28.5; IR (ATR) 3515, 3407, 3205, 1664, 1593, 1478, 1381, 1367, 1266, 1220, 1029, 798, 679 cm^{-1}.

6-Hydroxy-7-amino-4-methylcoumarin (1f) (knightletin). To an ice-cold solution of 110 mg (0.496 mmol) of **1e** in 1.5 mL of conc. NH_3 was added with stirring an ice-cold solution of 1.69 g (7.96 mmol) of 82% $Na_2S_2O_4$ in 7.5 mL of water. The reaction mixture rapidly changed color from red to yellow and, after stirring at 25°C for 3 h, the yellow solid that formed was collected by vac. filt. and dried to give 84 mg (88%) of **1f**: mp > 286°C (dec); ^{1}H NMR (500 MHz, d_6-DMSO) δ 6.90 (s, 1H), 6.57 (s, 1H), 5.95 (s, 1H), 4.86 (s, 3H), 2.34 (s, 3H); ^{13}C NMR (500 MHz, d_6-DMSO) δ 163.7, 154.8, 149.6, 142.8, 141.5, 109.4, 107.4, 106.8, 99.5, 17.3; IR (ATR) 3490, 3368, 3068, 1657, 1611, 1552, 1453, 1404, 1367, 1236, 1214, 1188, 938, 857, 828, 768, 563 cm^{-1}; HRMS (ESI) m/z $[M + H]^+$ calculated for $C_{10}H_{10}NO_3$: 192.0661 amu; found 192.0653 amu.

Results And Discussion

Absorbance and emission spectra, Stokes shift

Figure 1 shows the absorbance and emission spectra of knightletin in three solvents that vary in polarity and ability to hydrogen bond, EtOAc, MeCN and MeOH. These spectra show behavior that is consistent with the character of many other fluorescent coumarins. Table 1 gathers the fluorescence characteristics of knightletin and includes the Lippert solvent polarity parameter (orientation polarizability, Δf) [3, 7]. The Δf values show that EtOAc is significantly less polar than the other two solvents, while MeCN and MeOH are distinguished by the latter's ability to form hydrogen bonds. The fact that MeOH invokes a much larger red shift than MeCN suggests that hydrogen bonding influences the solvated ground electronic state. The significant absorbance red-shift due to MeOH has been observed in other 7-aminocoumarins [3, 17].

Table 1 Photophysical properties of knightletin in selected solvents, Lippert-Mataga bulk solvent polarity parameter, absorbance maximum wavelength, absorbance bandwidth, molar attenuation coefficient, fluorescence maximum wavelength, fluorescence emission bandwidth, Stokes shift, fluorescence quantum yield, observed fluorescence lifetime, and natural fluorescence lifetime.

Solvent	Δf	λ_a (nm)	abs-band FWHM (cm^{-1})	ε (M^{-1} cm^{-1})	λ_f (nm)	emis-band FWHM (cm^{-1})	SS (cm^{-1})	ϕ_f	τ_f (ns)	τ_f^0 (ns)
MeOH	0.309	370	4200	16	447	3000	4651	0.81	4.08	5.0
MeCN	0.305	358	4200	18	429	3100	4627	0.74	3.71	5.0
EtOAc	0.201	359	4100	16.5	423	3100	4258	0.71	3.44	4.8

The Stokes shift, which depends on both the absorbance and emission maximum wavelength, is also largest for MeOH indicating that specific hydrogen bonding interactions also play a key role in the electronic excited state. This is consistent with similar observations for many polar fluorophores [7]. Furthermore, the Stokes shift is well correlated with the solvent polarity parameter Δf like that observed for C120 in solutions of moderate to high polarity [3]. The slope of the Stokes shift versus Δf is like that of C120 indicating a similar sensitivity to solvent polarity. It is interesting to note that the knightletin Stokes shift of 4600 cm^{-1} in MeOH is considerably smaller than that for C120 (5800 cm^{-1}) and aesculetin (6000 cm^{-1}). The effect of the OH substitution in position 6 involves the electronic states due to its role in the molecular orbitals but will also influence the interaction with the solvent by affecting the molecular dipole moment and providing intermolecular hydrogen bonding with protic solvents.

Table 2 shows spectral properties of coumarins closely related to knightletin. The absorbance maximum wavelengths of knightletin are just outside the red end of the range of absorbance wavelengths of the

other coumarins in Table 2. C120 resembles knightletin only lacking the OH in position 6; like the relationship between umbelliferone (7-hydroxycoumarin) and aesculetin (6,7-dihydroxycoumarin). Scopoletin (6-methoxy-7-hydroxycoumarin) represents a similar coumarin that is also di-substituted on the benzene ring in the same positions as knightletin. Comparing C120 to knightletin in the three solvents, the absorbance of the latter shifts 15-20 nm to the red; the absorbance red shift from umbelliferone to aesculetin in MeOH is 25 nm. The Stokes shifts for knightletin are comparable to the range of values for other coumarins in Table 2 lying just outside the low end of that range.

Table 2 Reference photophysical characteristics of similar coumarins

Species	solvent	λ_a (nm)	ε (10^3 M^{-1} cm^{-1})	λ_f (nm)	SS (cm^{-1})	ϕ_f	τ_f (ns)	Ref.
knightletin	MeOH	370	16	447	4650	0.81	4.08	this work
aesculetin	MeOH	349	10	441	6000	0.18[a]	2.76[a]	this work
4-methyl-aesculetin	EtOH	341	–	410	4940	0.32	2.3	[18]
C120	MeOH	354	18.1[b]	434	5207	0.51	3.85	[3]
C120	MeCN	343	–	412	4880	0.63	3.10	[3]
		340		413	5200		4.35	[17]
C120	EtOAc	340	–	406	4781	0.62	2.90	[3]
scopoletin	MeOH	344	–	424	5500	–	2.67[c]	this work

a Ref [2]

b Ref [1]

c Ref [8]

Quantum yield

The quantum yield for knightletin in MeCN, determined relative to quinine sulfate, is 0.74 ± 0.04, making it about 15% more efficient than the commercial laser dye, C120, in MeCN. Figure S1 shows the knightletin/MeCN experimental decays and linear fits for the relative quantum yield determination. The emission spectra in Fig. 1 visually illustrate that MeOH has the largest quantum yield of the three solvents (at just over 80%) since the spectra are normalized to absorbance at the excitation wavelength

and scaled relative to the MeOH emission. Our observation that the knightletin quantum yield in both MeCN and EtOAc is about 10% lower than MeOH is the reverse of what is reported for C120 in the same set of solvents where the two aprotic solvents have ~20% larger quantum yield than for MeOH [3]. This may further point to an enhanced role for hydrogen bonding in the novel compound due to the additional hydroxy group. We also note that the knightletin quantum yield in MeOH is about four times larger than aesculetin in MeOH.

Time resolved fluorescence

The fluorescence lifetimes in Table 1 are from time resolved fluorescence decays of knightletin in the three solvents that are well represented by single exponential functions – see Figure S2 for fit details. The average fluorescence lifetime of around 4 ns is in good agreement with the range of 3 to 6 ns found in highly fluorescent coumarins. For example, 5 ns is the fluorescence lifetime of the anion in water of both scopoletin [8, 18] and umbelliferone [19]. The effect of different solvents on is consistent with the values in Table 2 by Pal et al. for C120 [3] with the least polar EtOAc having the lowest t and MeOH yielding the largest lifetime. Table 2 also shows that another study reports a C120/MeCN lifetime about 10% larger than our values for knightletin/MeCN, showing that the lifetimes are similar. The observed knightletin fluorescence lifetime and quantum yield combine to give a consistent natural lifetime, $\tau_f^0 = \tau_f/\phi_f$, of 5 ns.

Computational modeling

Modeling using a straightforward, DFT approach reveals key structural features of the novel knightletin molecule. The planar symmetry of the core coumarin structure leaves only the question of how the two benzene ring substituents interact. Hydroxyl group substitutions on the benzene are normally oriented along the plane, as is found in dihydroxy coumarins, such as aesculetin [2]. Orientation of the pyramidal amine group is more complex, but we can expect the vicinal hydroxyl and amine groups will interact forming a hydrogen bond (HB) with either N or O as the acceptor atom. Free of any coupling into delocalized molecular orbitals, we expect the OH donor HB (OH···N) to be stronger than the NH donor HB (NH···O). The report by David et al., giving the average energy of these specific hydrogen bonding interactions, indicates that OH···N is more than 3 times stronger than NH···O [20]. For comparison, a non-aromatic, vicinal amino and hydroxyl intramolecular interaction was modeled in 2-aminoethanol showing the gas-phase conformer with the OH donor HB is 8 kJ/mol lower energy than the corresponding conformer with NH donor HB using the same modeling level of theory applied to knightletin below – Figure S3 is a visualization of the 2-aminoethanol model.

Conformers

Describing conformers of knightletin requires a notation scheme where + or – indicates the orientation of the hydroxyl group in the molecular plane, pointing in the direction of decreasing numbers in the coumarin numbering scheme (Scheme 1), which we designate –, or towards increasing numbers,

designated +. The amine group orientation, as influenced by the expected HB formation, follows suit and is given the same sign as the OH. Thus, the conformer shown in Scheme 1 is the '– –' conformer with the NH acting as donor to the HB, and the '+ +' conformer has the opposite orientation with the OH acting as the HB donor. The +/– designation for the pyramidal NH_2 group can in some cases be ambiguous since the two bonds can have two kinds of symmetric orientation with respect to the coumarin plane, above and below the plane or both bonds on the same side of the plane. However, when the amine group is influenced by the vicinal OH group, the +/– notation is unambiguous to indicate the arrangement of the intramolecular hydrogen bond. To fully characterize the geometry of the substituent orientation, we define three dihedral angles involving NH or OH described in Scheme 3. Furthermore, the knightletin molecular structure has a classical Lewis-structure resonance represented in Scheme 4 in which the amine group is either pyramidal, structure I, or planar, II; modeling reveals structures that are between these limits where the C–N bond is between a single and double bond. As such, the C–N bond length is a proxy for the degree to which the amino group is coupled into the frontier molecular orbitals. Polar solvents tend to stabilize the charge transfer from amine to carbonyl, represented by the resonance structure on the right, shortening the C–N bond.

Our modeling reveals the KL– – conformer in the gas-phase is 4.8 kJ/mol lower energy than the KL+ + conformer indicating the NH donor configuration is more stable than the OH donor, the reverse of our expectation based simply on average HB strength. Substituent coupling into molecular orbitals must influence the orientation of the intramolecular HB.

Ground and first electronic state geometry

Table 3 collects selected geometric parameters for conformers of knightletin in the gas phase and in the three solvents. The hydrogen bond is represented by the hydrogen to acceptor atom distance. In the ground state of the – – conformer, the NH_2 group is pyramidal and has both NH bonds oriented on the same side of the coumarin plane as shown by the dihedral angles of around 20 degrees for both NH bonds. The N atom is slightly out of the coumarin plane – the dihedral N-C7-C6-C5 is 2.5° below the coumarin plane with H atoms on the other side of the plane. The amine group is twisted slightly, by less than 2°, towards the O atom possibly due to the presence of the HB. The d-OH dihedral is slightly out of plane by ~1° above the plane. Figure S4 is a visualization of the ground state knightletin – – conformer model illustrating the out-of-plane geometry. Our modeled NH_2 configuration in MeCN agrees well with the modeling of C120 [5] at a similar level of theory that shows a pyramidal NH_2 with corresponding dihedrals of 17.4° and –17.8° in MeCN.

Table 3 Geometric parameters and TD-DFT spectral results for conformers of knightletin at the B3LYP/cc-pVTZ level of theory and, where indicated the solvent is modeled using the SMD method; the dipole moment, dihedral angles (defined in Scheme 3), hydrogen bond length (H atom to acceptor atom distance), and NC bond length are from the optimized geometry, the wavelength and intensity are from TD-DFT results (see text); ground state is shaded rows, the + + conformer data are in italics

Conformer, electronic state	surroundings	μ (D)	d-NH_b (°)	d-NH_f (°)	d-OH (°)	D_{H-A} (Å)	D_{NC} (Å)	λ (nm)	Int.
−−, S_0	vacuum	6.83	18.8	–22.2	1.2	2.285	1.377	329.5	0.301
−−, S_1	vacuum	7.07	0	0	0	2.358	1.369	366.7	0.263
++, S_0	*vacuum*	*5.55*	*51.3*	*–4.6*	*–149.1*	*2.342*	*1.402*	*323.6*	*0.227*
++, S_1	*vacuum*	*4.12*	*–61.1*	*61.1*	*0*	*2.023*	*1.432*	*409.9*	*0.094*
−−, S_0	MeOH	10.8	21.3	–19.5	–1.6	2.323	1.370	348.7	0.426
−−, S_1	MeOH	12.2	0.03	–0.03	0	2.361	1.348	409.2	0.678
−−, S_0	MeCN	9.62	21.3	–19.9	1.8	2.324	1.371	343.9	0.411
−−, S_1	MeCN	10.7	0.08	–0.05	0	2.373	1.351	400.6	0.633
−−, S_0	EtOAc	8.86	20.1	–20.3	1.7	2.309	1.372	341.8	0.415
−−, S_1	EtOAc	9.61	8.5	–8.6	–0.4	2.365	1.357	388.6	0.534

Our modeled ground state configuration (knightletin − −) can be compared to 2-aminophenol (2AP), which has the same vicinal substituents coupled by the resonance of the benzene ring. The recent work of Capello et al. gives both experimental and theoretical results for jet-cooled gas-phase 2AP [21]. They report IR-UV hole burning action spectra showing IR features corresponding to NH symmetric and antisymmetric stretches and an OH stretch of 3669 cm^{-1} clearly indicating the OH is not involved in an intramolecular HB, a so-called 'free' OH stretch. This OH stretch is red-shifted from the OH stretch of MeOH(*g*) of 3681 cm^{-1} [22], showing that the context of being bound to the benzene ring and vicinal to NH_2 does influence the OH vibrational frequency even when 'free.' The Capello data supports the 2AP conformer that corresponds to knightletin − −. Their modeling, which is at a higher level of theory than our approach, indicates the two 2AP conformers are nearly isoenergetic (favoring the free OH conformer when zero-point energy is considered) agreeing well with our own modeling of 2AP predicting the free OH conformer as more stable by less than 1 kJ/mol. And yet, the 2AP experimental data clearly points to favoring the conformer with the un-bound OH, rather than a gas-phase mixture of the two conformers. Interestingly, the Capello account of the observed 2AP conformer describes the NH···O HB as nonexistent, which raises the question to what extent the study of knightletin will reveal the impact of the NH···O HB in the knightletin − − conformer. Further modeling work will help in that regard, for example to study rotational barriers. We note the IR-action spectroscopic study by Carrascosa et al. on the cryogenically cooled aesculetin-H^+ cation [23] shows that it is possible to observe gas-phase IR action spectra of substituents on coumarins similar to knightletin.

In our modeling of the knightletin excited state geometry in the gas phase, the NH_2 group is planar for the optimized − − conformer. Figure 2 shows the gas-phase frontier orbitals revealing a charge transfer of HOMO electron density located on the benzene ring shifting to the pyrone ring in the LUMO, which is

consistent with favoring planar geometry in the excited state. The HOMO to LUMO transition accounts for 94% of the molecular orbitals contributing to the calculated first electronic excitation. The observation that the dipole moment increases upon excitation to the LUMO also fits with a charge transfer interpretation. The planar NH_2 geometry is fully realized in the gas phase (dihedral angles equal zero) and this planar geometry is approached in solution as the solvent polarity increases. Also concordant, the C–N bond length becomes shorter with the transition to the electronic excited state and increasing solvent polarity.

It is interesting to note that the higher energy ground state knightletin + + conformer exhibits a potential double HB because the OH orientation puts the H atom 2.342 Å from the N acceptor, while the H atom in NH_b is oriented towards the O atom and is 2.608 Å from the O acceptor. Figure S4 is a visualization of the ground state knightletin + + conformer model. It is also worth noting that the optimized excited state geometry of the + + conformer is lower in energy than the optimized excited state – – conformer by 12 kJ/mol, thus the modeling suggests the potential for excited state dynamics involving reversing the hydrogen bond upon excitation of the – – conformer. The supplemental information contains the gas phase XYZ coordinates for the optimized ground state and first electronic excited state of both knightletin conformers.

Calculated spectroscopic properties

Table 3 also shows the results from applying TD-DFT methods to predict absorbance and fluorescence characteristics of knightletin. In general, the model underestimates the absorbance and fluorescence maximum wavelengths in the solvents by an average of 18 and 34 nm, respectively, but the shift to longer wavelengths with increasing polarity matches experiment. The calculated Stokes shift is low by about 10% compared to experiment, but again the observed increase in Stokes shift with increasing solvent polarity is reproduced in the model. Zhao argues for C120 modeling that some of the spectral mismatches in protic solvents are due to lack of explicit hydrogen bonding in the model [5], a claim that is worth further investigation for knightletin.

Other modeled molecular properties

For knightletin, the anion formed by removal of the OH proton is lower energy compared to the anion with the NH proton removed, predicting that deprotonation will occur at position 6. This is consistent with our preliminary estimate of the pK_a for knightletin described in the next section on future study. Calculating the pK_a of di-substituted coumarins is the subject of a current study in our lab.

The presence of the intramolecular hydrogen bond may influence the ability of the NH_2 group to rotate, which in turn may influence the fluorescence quantum yield. Flexibility of the amino group in aminocoumarin laser dyes is tied directly to the so-called TICT state (twisted intramolecular charge transfer) associated with compromised fluorescence quantum yield [10]. Efforts to inhibit amino group

rotation by addition of bulkier ethyl groups or inclusion of cyclic molecular structures are shown to improve the quantum yield [10].

The Zhao study [5] emphasizes the need for including explicit water molecules in modeling of the absorbance spectra. Knightletin represents another important molecular example that now includes an intramolecular HB for testing the ability of models to describe spectroscopic characteristics of coumarins.

Future study

A key question is how knightletin behaves as a weak acid and perhaps as a photoacid like aesculetin, which has been shown to be one of the strongest photoacids of the natural coumarins [2]. Preliminary studies point to knightletin having a pK_a ~9, which is like the pK_a of grevillone (6-hydroxycoumarin) [24], where the only ionizable proton is in position 6. Studying knightletin in a broader spectrum of solvents may reveal more molecular details and physical properties, although we note that knightletin does not readily dissolve in cyclohexane. Studies will include water and water/alcohol mixtures to observe solvent and pH effects on absorbance and fluorescence properties. Further elucidation of the role of hydrogen bonding in knightletin is a key goal.

Conclusion

Knightletin is a novel coumarin, which exhibits intramolecular hydrogen bonding between the vicinal amino and hydroxyl groups on the benzene ring. It has a high quantum yield that exceeds C120 suggesting the presence of OH modestly improves the quantum yield. The compound also provides an interesting comparison to aesculetin, recently shown to be a very strong photoacid, pointing to further investigation of the acid and anionic character of knightletin.

Statements And Declarations

Acknowledgements

The authors are grateful for the following support: We thank Dr. Gary Blanchard, Michigan State University, for his generous time, collaboration and providing access to his TRF system. The MSU Mass Spectrometry and Metabolomics Core provided LC-high resolution mass spec data.

Funding – National Science Foundation grant 1956223, Beckman Scholars Program (LK), NSF-funded Calvin Computer cluster (MRI-grant 1726260), Calvin Research Fellowship program (MM), Luke and Pauline Schaap Summer Research Fellowship (GD), the Thedford P. Dirkse Summer Science Research Fellowship (IJ), Calvin Honors Program (ED)

Conflicts of interest/Competing interests – the authors declare no conflicts of interest or competing interests

Authors' contributions – LK edited the draft for general write up and performed experiments and modeling, ED and GD performed DFT modeling, IJ performed the experiments, LH performed the experiments and assisted with synthesis, RB performed the synthesis, MM wrote the manuscript in consultation with the other co-authors.

Data availability – All data generated or analyzed during this study are included in this published article and its supplementary information

Ethics approval/declarations – not applicable

Consent to participate – not applicable

Consent to publish – not applicable

Code availability – not applicable

References

1. Brackmann U (2000) Lambdachrome(R) Laser Dyes, Third edition. Lambda Physik AG, Goettingen · Germany
2. Knoor ALH, Du Laney GR, Jonker IB et al (2022) Aesculetin Exhibits Strong Fluorescent Photoacid Character. J Fluoresc 32:307–318. https://doi.org/10.1007/s10895-021-02842-w
3. Pal H, Nad S, Kumbhakar M (2003) Photophysical properties of coumarin-120: Unusual behavior in nonpolar solvents. J Chem Phys 119:443–452. https://doi.org/10.1063/1.1578057
4. Moog RS, Kim DD, Oberle JJ, Ostrowski SG (2004) Solvent Effects on Electronic Transitions of Highly Dipolar Dyes: A Comparison of Three Approaches. J Phys Chem A 108:9294–9301. https://doi.org/10.1021/jp0486088
5. Zhao W, Pan L, Bian W, Wang J (2008) Influence of Solvent Polarity and Hydrogen Bonding on the Electronic Transition of Coumarin 120: A TDDFT Study. ChemPhysChem 9:1593–1602. https://doi.org/10.1002/cphc.200800131
6. Vanden Broeck A, McEwen AG, Chebaro Y et al (2019) Structural Basis for DNA Gyrase Interaction with Coumermycin A1. J Med Chem 62:4225–4231. https://doi.org/10.1021/acs.jmedchem.8b01928
7. Lakowicz JR (2006) Principles of Fluorescence Spectroscopy. Springer US. 3rd edn.https://doi.org/10.1007/978-0-387-46312-4
8. Pham HT, Yoo J, VandenBerg M, Muyskens MA (2020) Fluorescence of Scopoletin Including its Photoacidity and Large Stokes Shift. J Fluoresc 30:71–80. https://doi.org/10.1007/s10895-019-02471-4
9. Quaranta M, Murkovic M, Klimant I (2013) A new method to measure oxygen solubility in organic solvents through optical oxygen sensing. Analyst 138:6243–6245.

https://doi.org/10.1039/c3an36782g

10. Jones G, Jackson WR, Choi CY, Bergmark WR (1985) Solvent effects on emission yield and lifetime for coumarin laser dyes. Requirements for a rotatory decay mechanism. J Phys Chem 89:294–300. https://doi.org/10.1021/j100248a024
11. Frisch M, Trucks G, Schlegel H et al (2016) Gaussian 16, Revision B.01. Gaussian, Inc., Wallingford, CT
12. Schmidt J, Polik W, WebMO Pro WebMO, LLC, Holland, MI, USA. Available from http://www.webmo.net
13. Marenich AV, Cramer CJ, Truhlar DG (2009) Universal Solvation Model Based on Solute Electron Density and on a Continuum Model of the Solvent Defined by the Bulk Dielectric Constant and Atomic Surface Tensions. J Phys Chem B 113:6378–6396. https://doi.org/10.1021/jp810292n
14. Kaufman KD, McBride DW, Eaton DC (1965) Synthetic Furocoumarins. VII. Oxazolocoumarins from 6-Hydroxy-4-methylcoumarin. J Org Chem 30:4344–4346. https://doi.org/10.1021/jo01023a524
15. Mewada GS, Shah NM (1956) Die Nitrierung des 6-Hydroxy-4-methyl-cumarins und seines Methyläthers. Chem Ber 89:2209–2211. https://doi.org/10.1002/cber.19560890924
16. Ganguly NC, Datta M, De P, Chakravarty R (2003) Studies on Regioselectivity of Nitration of Coumarins with Cerium(IV) Ammonium Nitrate: Solid-State Nitration of 6-Hydroxy-Coumarins on Montmorillonite K-10 Clay Support Under Microwave Irradiation. Synth Commun 33:647–659. https://doi.org/10.1081/SCC-120015821
17. Rechthaler K, Köhler G (1994) Excited state properties and deactivation pathways of 7-aminocoumarins. Chem Phys 189:99–116. https://doi.org/10.1016/0301-0104(94)80010-3
18. Pina J, de Castro CS, Delgado-Pinar E, Sérgio Seixas de Melo J (2019) Characterization of 4-methylesculetin and of its mono- and di-methoxylated derivatives in water and organic solvents in its ground, singlet and triplet excited states. J Mol Liq 278:616–626. https://doi.org/10.1016/j.molliq.2019.01.083
19. Simkovitch R, Huppert D (2015) Photoprotolytic Processes of Umbelliferone and Proposed Function in Resistance to Fungal Infection. J Phys Chem B 119:14683–14696. https://doi.org/10.1021/acs.jpcb.5b08439
20. David V, Grinberg N, Moldoveanu SC (2018) Long-Range Molecular Interactions Involved in the Retention Mechanisms of Liquid Chromatography, Chap. 3. In: Advances in Chromatography. pp 73–110
21. Capello MC, Broquier M, Ishiuchi S-I et al (2014) Fast Nonradiative Decay in o-Aminophenol. J Phys Chem A 118:2056–2062. https://doi.org/10.1021/jp411457v
22. Shimanouchi T (1972) Tables of Molecular Vibrational Frequencies, Consolidated Volume 1. National Bureau of Standards
23. Carrascosa E, Pellegrinelli RP, Rizzo TR, Muyskens MA (2020) Cryogenic Infrared Action Spectroscopy Fingerprints the Hydrogen Bonding Network in Gas-Phase Coumarin Cations. J Phys Chem A 124:9942–9950. https://doi.org/10.1021/acs.jpca.0c06430

24. Nowak PM, Woźniakiewicz M, Piwowarska M, Kościelniak P (2016) Determination of acid dissociation constant of 20 coumarin derivatives by capillary electrophoresis using the amine capillary and two different methodologies. J Chromatogr A 1446:149–157. https://doi.org/10.1016/j.chroma.2016.03.084

Schemes

Schemes 1-4 are available in the Supplementary Files section.

Figures

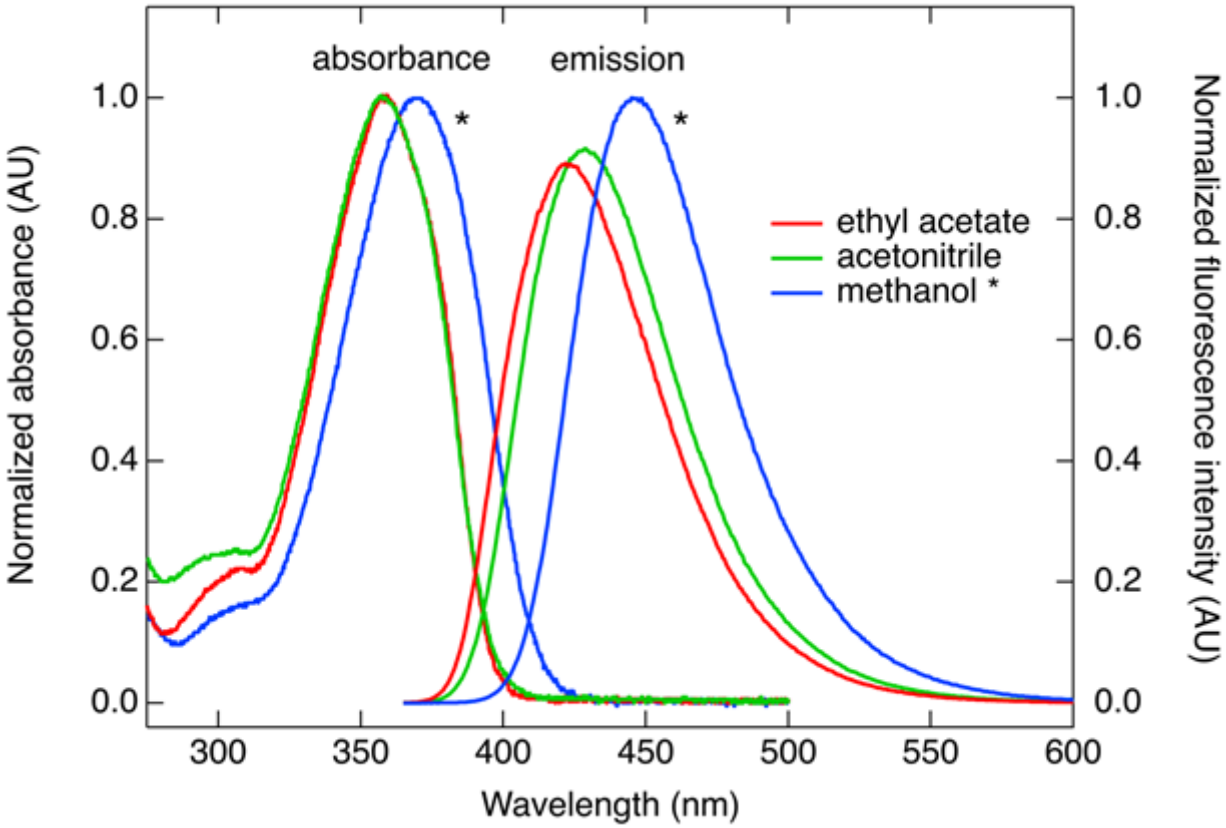

Figure 1

Normalized absorbance and emission spectra for knightletin in EtOAc (red), MeCN (green), and MeOH (blue, starred), 9 μM; emission spectra are excited at 350 nm, normalized to absorbance at 350 nm and areas scaled relative to the integrated MeOH emission intensity; the star disambiguates the figure when viewed in B&W

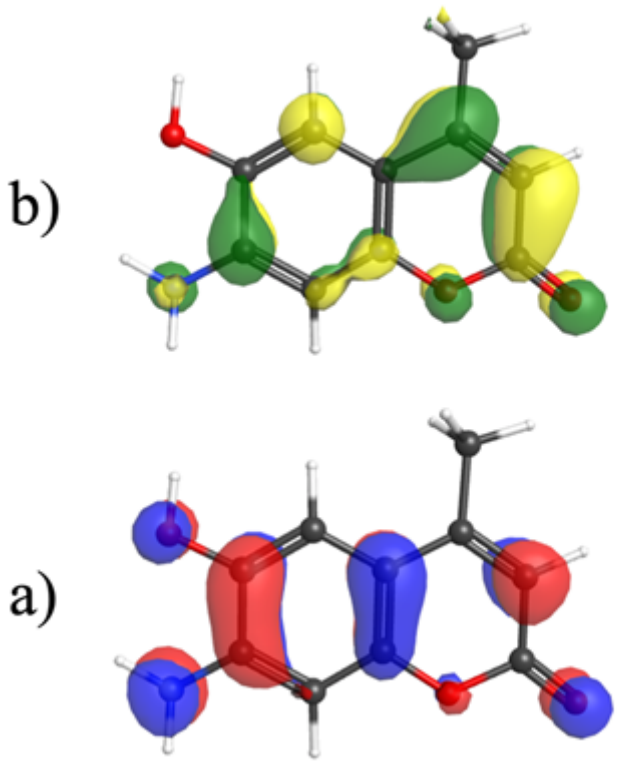

Figure 2

Molecular orbitals for gas-phase knightletin – – conformer modeled at the B3LYP/cc-pVTZ level of theory, (a) is the highest occupied MO and (b) is the lowest unoccupied MO

Supplementary Files

This is a list of supplementary files associated with this preprint. Click to download.

- SupplementalinformationforKLmanuscript3may22submitted.docx
- Scheme1.png
- Scheme2.png
- Scheme3.png
- Scheme4.png